Trophic interactions decouple soil carbon temperature response from that of microbial decomposers

Benjamin N. Sulman[1] and Jean P. Gibert[2]

1. Environmental Sciences Division and Climate Change Science Institute, Oak Ridge National Laboratory, Oak Ridge, TN, USA, sulmanbn@ornl.gov
2. Department of Biology, Duke University, Durham, NC, USA, jean.gibert@duke.edu

Corresponding author:
Benjamin N. Sulman
Mail: P.O. Box 2008, MS6301, Oak Ridge, TN 37831, USA
Phone: (865) 576-0766
Fax: (865) 241-4088
Email: sulmanbn@ornl.gov

Statement of authorship: Both authors conceived the study, designed and conducted the mathematical modeling, analyzed and interpreted the results, and wrote the paper.

Data accessibility: All model code, driver data, and output are available at https://github.com/JPGibert/Microbial_munchers

Keywords: Soil, carbon, climate change, warming, food webs, modeling, trophic interactions

Notice: This manuscript has been authored by UT-Battelle, LLC, under contract DE-AC05-00OR22725 with the US Department of Energy (DOE). The US government retains and the publisher, by accepting the article for publication, acknowledges that the US government retains a nonexclusive, paid-up, irrevocable, worldwide license to publish or reproduce the published form of this manuscript, or allow others to do so, for US government purposes. DOE will provide public access to these results of federally sponsored research in accordance with the DOE Public Access Plan (http://energy.gov/downloads/doe-public-access-plan).

Abstract

Soil organic carbon (SOC) stocks represent a large component of the global carbon cycle that is sensitive to warming. Modeling and empirical studies often assume that temperature responses of microbial physiological functions and extracellular enzymatic reactions are predictive of ecosystem-scale SOC decomposition responses to warming. However, temperature-dependent soil trophic interactions such as predation of microbial decomposers by other organisms have not yet been incorporated into quantitative SOC models. Here, we incorporated a microbial predator into a tri-trophic population ecology model and a global-scale predictive SOC model to determine how predation would affect soil community population dynamics and temperature sensitivity of SOC stocks. Predators increased SOC stocks and their dependence on substrate input rates. Top-down controls of predators on microbial biomass caused SOC warming responses to diverge from microbial temperature responses, with warming-induced SOC losses reduced or reversed when predators were more temperature-sensitive. Our results suggest that higher trophic levels can reduce the sensitivity of SOC to warming, and that differences in temperature sensitivity across trophic levels may be a key determinant of SOC warming responses.

Introduction

Understanding how rapid global climate change may impact the structure and dynamics of food webs and associated ecosystem-level processes and services is a pressing but challenging issue in ecology. An important but often overlooked component of ecological dynamics lies beneath the ground in the form of soil food webs. Soils represent the largest cycling terrestrial carbon (C) pool on earth [1]. While soil organic carbon (SOC) stocks are thought to be vulnerable to warming [2], projected responses of SOC stocks to climate change are highly uncertain [3,4] and measured responses of SOC to warming have been inconclusive [5,6]. Recent work explicitly incorporating biological processes into SOC models [7] highlights important mechanisms and related uncertainties in SOC cycling, including differences in microbial carbon use efficiency (CUE) and its temperature sensitivity [8,9], rhizosphere priming effects [10], microbial dormancy [11,12], and density-dependent microbial biomass turnover [13]. Microbial processes are thus increasingly recognized as a major determinant of SOC stocks and are now being incorporated into global-scale studies of climate change impacts on soil C stocks [3,10,14,15], facilitating the incorporation of these processes into earth system model (ESM) projections of terrestrial C cycle responses to global climate change.

SOC models using explicit microbial processes have also produced seemingly unrealistic results like oscillations in SOC stocks and insensitivity to carbon input rates [16]. While model structures can mitigate these issues [10,13,17], variations in assumptions and parameterizations can drive wide differences in projected responses to ecosystem perturbations [6]. At the same time, measurements of microbial physiological and phylogenetic traits can be used to directly constrain model parameters [8,18,19]. Recent reviews have suggested that incorporating metagenomics information into microbial-explicit soil decomposition model parameterizations could improve model projections of SOC responses to changing environmental conditions [20–22]. To date, however, microbial-explicit SOC models have focused on the role of a single category of living organisms in the soil: microbial decomposers [7]. Such models, along with laboratory and field measurements of microbial physiological traits, however, may not completely reflect ecosystem dynamics if they ignore interactions with other components of the soil food web.

The role of trophic interactions

While microbial-explicit SOC models have yielded important insights about decomposition processes, other important mechanisms, such as trophic interactions between microbes and other organisms in the soil food web, have so far been excluded [23–27]. Food web structure can drive ecosystem dynamics in both terrestrial and aquatic systems [28]. Moreover, trophic interactions are temperature-dependent through physiological responses [29–31], changes in animal movement [32], and other trait responses to temperature [33–35]. For example, predation pressure on eel sea grass beds varies with temperature along latitudinal gradients [36], climate influences predator-prey ratios in bromeliad communities [37] and warming increases the strength of plant-herbivore interactions [38]. Trophic interactions can also alter SOC decomposition: the presence of microbe-eating isopods changes SOC responses to global change [39], grazing on microbes by organisms at higher trophic levels impacts microbial growth patterns [40], litter decomposition and C utilization vary with soil faunal community complexity [41], and interactions between predatory spiders and fungivorous Collembola change with warming to reduce litter decomposition [42]. Together, these results suggest important but largely overlooked interactions between warming, trophic interactions and SOC responses. Food web structure

and dynamics are susceptible to changes in temperature [43–45], but understanding of how food webs mediate the effects of temperature on decomposition, and the integration of these principles into SOC models, have so far been limited [23,46].

Integrating trophic interactions into SOC models is challenging due to the complexity of soil food webs and the difficulty of obtaining measurements that can constrain model parameters [47]. However, recent studies using microbial-explicit SOC models have demonstrated that biological interactions can be integrated into tractable models and can drive important differences in projected outcomes compared to models that treat biological processes implicitly [7,23,46]. To address these issues, and as a first step toward integrating food web interactions into quantitative SOC models, we developed two models of soil trophic interactions including SOC, microbial decomposers, and predators that feed on microbes. First, we modified a population ecology predator-prey model to demonstrate conceptually how soil microbe predators may determine SOC responses to temperature. Second, we modified a state-of-the-art, quantitative SOC cycling model – the Carbon Organisms Rhizosphere and Protection in the Soil Environment (CORPSE) model [10] – to show how incorporating microbe predators into simulated soil food webs impacts SOC projections under warming across gradients of climate and ecosystem productivity at a global scale. Given the premise that loss of SOC in response to warming is accelerated by microbial growth and SOC assimilation, we test the hypothesis that the presence of a higher trophic level that consumes microbial decomposers weakens the connection between the temperature sensitivity of microbial substrate consumption and the temperature sensitivity of SOC stocks. In addition, we evaluate the importance of local adaptation and differences in temperature sensitivity across trophic-levels in determining latitudinal patterns of these trophic interactions and their effects on SOC stocks.

Methods:

Trophic-chain food web models

The simplest approach to modeling SOC decomposition only considers carbon stock (C) naturally decaying over time at a temperature-dependent first-order rate k (Fig 1A) while being replenished at a constant rate I (Supplementary Information, eq S1). While global land surface models such as those used in the Climate Model Intercomparison Project Phase 5 (CMIP5) comparison predominantly use multiple-pool versions of this approach [48], studies [7] have suggested that model fidelity can be improved by explicitly simulating microbial biomass as the driver of decomposition (Fig 1B). We model the microbial effect on carbon as a classic type-II functional response, where the SOC decomposition rate depends on microbial biomass and carbon stocks (M and C, respectively), as well as on two parameters controlling the feeding process, the microbial attack rate (α) and handling time η [49,50]. Conversion of carbon into microbial biomass is determined by a conversion efficiency parameter (ε), and microbes die naturally at a per-capita rate d_M (SI, eqs S2 and S3). Microbial attack rates are temperature-dependent, following an Arrhenius function of the form:

$$\alpha(T) = Ve^{-\frac{E_a}{k_b}\left(\frac{1}{T}-\frac{1}{T_0}\right)}, \quad (1)$$

where V is a pre-exponential rate constant (units of inverse time), k_b is the Boltzmann constant ($8.62\text{x}10^{-5}$ electron-volts per degree Kelvin, eV K^{-1}), T is the temperature at which the process occurs (in K), T_0 is a

reference temperature (K), and E_a is the activation energy of the process (in eV), which is a measure of its temperature dependence [30,32,51].

To incorporate the effects of a microbial predator, we added a third trophic level, *P*, that preys on the microbial biomass, *M*, also following a type II functional response with an attack rate following the same temperature response as that of microbial biomass (Eq. 1). This microbe-predator model (Fig 1C) makes similar assumptions as the microbial model, and can thus be written as:

$$\frac{dC}{dt} = I - \frac{\alpha_1(T)CM}{1+\alpha_1(T)\eta_1 C} \quad (2)$$

$$\frac{dM}{dt} = \varepsilon_1 \frac{\alpha_1(T)CM}{1+\alpha_1(T)\eta_1 C} - \frac{\alpha_2(T)MP}{1+\alpha_2(T)\eta_2 M} \quad (3)$$

$$\frac{dP}{dt} = \varepsilon_2 \frac{\alpha_2(T)MP}{1+\alpha_2(T)\eta_2 M} - d_P P \quad (4)$$

For both microbe and microbe-predator models, steady-state solutions were found analytically. We determined solutions across a range of substrate inputs and temperatures and further analyzed model behavior using Wolfram Mathematica 11 (code available at https://github.com/JPGibert/Microbial_munchers). Parameter values used in our analyses are shown in Table S1 and were chosen so that equilibrium biomass in all non-warmed scenarios showed a regular biomass pyramid (*C*>*M*>*P*).

Quantitative SOC models

While the modeling approach described above illustrates the dynamical effects of an additional trophic level on microbe populations and SOC concentrations (Fig 1A), it was not designed to quantitatively reproduce observed SOC stocks or organismal biomass in soils, or to represent key mechanisms in soil biogeochemical cycling such as stabilization of SOC through physico-chemical interactions with minerals [52]. To incorporate the trophic interactions identified in the food web models into a quantitative SOC framework, we implemented a predator trophic level in the Carbon Organisms Rhizosphere and Protection in the Soil Environment (CORPSE) model, which includes SOC and microbial decomposer pools and has been previously applied and validated against measurements at both ecosystem and global scales [3,10,53]. Here, we refer to the modified model as CORPSE-Pred. CORPSE-Pred differs from the food web model in key aspects. First, CORPSE-Pred divides substrate C into multiple types representing simple, complex, and microbial-biomass-derived compounds. Second, microbial and predator populations in CORPSE-Pred are constrained not to decline below a minimum value, preventing their complete eradication. Third, decomposition and predation kinetics in CORPSE-Pred are calculated using the ratio of microbe to SOC carbon, or the ratio of predator to microbe carbon, rather than the absolute stocks or concentrations of those factors (an equivalent formulation in the predator-prey models would be to include ratio-dependent foraging rates or interference competition). Under these assumptions, changes in carbon stocks, C, over time can be calculated as:

$$\frac{dC_i}{dt} = I_i - V_i e^{-\frac{E_{a_i}}{k_b}\left(\frac{1}{T}-\frac{1}{T_0}\right)} \times \theta^a (1-\theta)^b k_\theta \times C_i \frac{M}{M+k_M C}, \quad (5)$$

where C_i is substrate carbon of type i (representing chemical classes with different decomposition rates and microbial CUEs), I_i is input rate of each substrate type, θ is volumetric soil water content as a fraction of saturation, a and b control moisture sensitivity of decomposition, k_θ is a normalization constant for moisture sensitivity, M is microbial biomass, and k_M controls the relationship between microbial biomass and decomposition rate. The temperature dependence of the interaction between C and the microbes was modeled using Eq. 1 but with substrate-specific parameters, where V_i is the maximum microbial decomposition rate of substrate type i, and Ea_i is the activation energy for decomposition of each substrate type. Inputs (I) include a fraction (60%) of microbial and predator death (excluding microbial biomass loss from predation). The rate of change of the microbial biomass, M, can be modeled by:

$$\frac{dM}{dt} = \sum_i([V_i e^{-\frac{Ea_i}{k_b}(\frac{1}{T}-\frac{1}{T_0})} \times \theta^a(1-\theta)^b k_\theta \times C_i \frac{M}{M+k_M C}] \times \varepsilon_i) - (M - M_{min}\sum_i C_i) \cdot d_M - V_P e^{-\frac{Ea_P}{k_b}(\frac{1}{T}-\frac{1}{T_0})} \cdot M \frac{P}{P+k_P M}, \quad (6)$$

where ε_i is microbial carbon use efficiency associated with each substrate type, $B_{M,min}$ is the minimum microbial biomass (expressed as a fraction of total substrate C), d_M is the background death rate for microbial biomass, V_P is maximum predation rate, Ea_P is the activation energy parameter for predation, and k_P is a parameter controlling the relationship between predation and predator biomass. Finally, the rate of change of predator biomass can be modeled as:

$$\frac{dP}{dt} = \varepsilon_P[V_P e^{-\frac{Ea_P}{k_b}(\frac{1}{T}-\frac{1}{T_0})} \times M \frac{P}{P+k_P M}] - (P - P_{min} M) \cdot d_P, \quad (7)$$

where ε_P is carbon use efficiency of predators, P_{min} is minimum predator biomass, and d_P is death rate of predators. CORPSE-Pred also includes protected SOC stocks that are inaccessible to decomposition. We do not show the equations for protected SOC here for brevity (see SI for full model equations including those related to protected SOC).

We drove global SOC simulations using 10 years of monthly-average net primary production (NPP), soil temperature, and soil moisture from previous global simulations using the Geophysical Fluid Dynamics Laboratory (GFDL) global land model LM3 [54,55]. NPP was assumed to be equivalent to total carbon inputs to soil (thereby assuming plant biomass was at approximate steady state). Meteorological forcing for the LM3 simulations used a gridded historical climate dataset over years 1958-1967 [56], which were repeated to drive simulations of any length. We numerically integrated the CORPSE-Pred model for 750 years to equilibrate all pools, then conducted control simulations and warming simulations with temperatures increased by 2 ºC.

We conducted CORPSE-Pred simulations using two alternative assumptions concerning local temperature adaptation of predator physiology. With local adaptation, T_0 for predators was set to the control simulation mean annual temperature of each grid cell. With globally constant base temperature, T_0 for predators in each grid cell was equal to the mean global temperature (13 ºC).

CORPSE-Pred simulations used parameter values from previous CORPSE simulations [10,57] where possible. Values of new parameters associated with predation-related processes were chosen to reproduce the same approximate global patterns under steady-state conditions but could not be further constrained due to the paucity of measurements directly comparable to model trophic levels. Parameters and values are shown in Table S2. Simulations were conducted at a five-day time step using an implementation of the model in python. Scripts, model code, forcing data, and model output are available at the aforementioned github repository.

Characterization of SOC temperature responses

To compare the temperature response of SOC stocks with the temperature dependence of microbe and predator growth rates, we used changes in SOC stocks under warming to calculate an equivalent SOC temperature sensitivity (CE_a) in the same units as the temperature-dependence parameters in our models (Ea), following an approach previously used to estimate equivalent Q_{10} values [58]. SOC temperature dependence can be approximated as:

$$SOC_T = SOC_{T_0} e^{-\frac{CE_a}{k_b}\left(\frac{1}{T}-\frac{1}{T_0}\right)}, \quad (8)$$

where SOC_T and SOC_{T_0} are carbon stocks at temperatures T and T_0 respectively. This relationship can be solved for CE_a:

$$CE_a = k_B \ln\left(\frac{SOC_T}{SOC_{T_0}}\right)\left(\frac{1}{\frac{1}{T}-\frac{1}{T_0}}\right). \quad (9)$$

CE_a represents the temperature sensitivity that would result in a given ratio of SOC stocks at steady state under two different temperatures. Assuming SOC stocks have approached a steady state following any temperature perturbation, CE_a values can be compared across simulations with different assumptions to quantify differences in SOC temperature responses.

Results:

Trophic-chain food web models

The population-based microbial model illustrated the fundamental impact of a third trophic level on SOC dynamics. A two-level model, including only substrate and microbial decomposers, reproduced dynamics shown in previous microbial decomposition models [16]: steady-state SOC was independent of substrate input rates (I) while microbial biomass increased with I (Figure 2a). Warming reduced SOC concentration but did not affect microbial biomass. Adding a third trophic level fundamentally changed SOC dynamics (Figure 2b). With predators, SOC increased at an accelerating rate with greater I while microbial biomass was constant with respect to I. Predator biomass did not persist below a minimal I. Warming decreased SOC stocks while increasing microbial and predator biomasses.

SOC warming sensitivity varied with the relative temperature-dependence of microbes and their predators (E_a, Figure 2c). When microbes were more temperature-sensitive than their predators, warming depleted SOC. Above a critical predator E_a, reduction of microbial biomass due to increased predation drove accumulation rather than loss of SOC under warming. The strength of this effect depended on substrate input rate, such that an increase in substrate inputs led to a larger effect of differences in temperature dependence across trophic levels (SI Fig S1).

When the two models (with and without predation) were directly compared, the temperature sensitivity of SOC stocks in the presence of predators (CE_a) decreased compared to that of a model without predators, suggesting a weaker temperature dependence of SOC stocks in the presence of predators (Fig 2d). The difference in SOC temperature sensitivities between the two and three-level models was itself temperature dependent and increased with warming. The magnitude of the reduction in SOC temperature sensitivity

due to predators was determined by the relative temperature sensitivity of microbes and predators: increasing predator Ea reduced the temperature sensitivity of SOC when predators were present (Fig 2d).

Quantitative global SOC model

We used global simulations with the CORPSE-Pred model to investigate how predator activity would alter SOC responses to warming across gradients of climate and ecosystem productivity. CORPSE-Pred reproduces the key aspects of top-down control of microbial populations via predation predicted in the population-based approach (Fig. S2) as well as the effects of variable temperature sensitivities across trophic levels (Fig. S3) suggesting a fundamental level of agreement between both modeling approaches despite differences in model structure and assumptions. However, the structure of CORPSE-Pred facilitated simulations across large gradients of mean annual temperature and C inputs, allowing the investigation of microbe-predator interactions on SOC stocks across climate gradients, and facilitating comparison of alternative assumptions regarding local adaptation of predator populations.

Predator effects across latitudes

Variation in predator biomass across latitudes depended on alternative assumptions of local adaptation. With locally-adapted predator T_0, predator populations were significant across tropical, temperate, and boreal climate zones (Figure 3a). These larger populations led to significant top-down control on microbial populations, reducing microbial biomass by 10-20% in the tropics and by over 50% in higher latitudes (Figure 3b) relative to simulations without predators. By contrast, a globally constant T_0 led to higher predator populations in the tropics and lower populations in high latitudes (Figure 3c). Under this assumption, top-down control on microbial biomass was enhanced in the tropics and much weaker in high latitudes (Figure 3d).

With no predators, SOC temperature sensitivity (CE_a) varied moderately across latitude, with higher values (around 0.6 eV) in high latitudes and lower values (around 0.3 eV) in the tropics (Figure 4a). This variation was most likely due to the effect of protected C stocks that were not directly responsive to warming but still exchanged C with unprotected SOC pools. Predators lowered CE_a globally, indicating weaker temperature responses due to top-down control on microbial biomass. In the tropics, CE_a was reduced to about 0.2 eV with both locally-adapted and global constant predator T_0. With globally constant predator T_0, CE_a was reduced by about the same amount in high latitudes (Fig. 4c). However, with locally adapted predator T_0, CE_a in high latitudes was more strongly reduced, reaching negative values across northern areas that indicated a reversed temperature dependence with SOC stocks increasing under warming (Fig. 4b). Negative CE_a values occurred in desert regions with globally constant T_0, but SOC stocks were low in those regions under all conditions.

Discussion

Implications for SOC stocks and warming responses

Both the population-based and the quantitative modeling approaches suggested that higher trophic levels and their temperature dependence can strongly affect SOC stocks and their warming responses. Introducing a third trophic level in food web models also caused SOC to become dependent on the rate of substrate inputs, thus resolving a known flaw of some microbial-explicit SOC model formulations [16,17]. Our results thus suggest that top-down control of microbial biomass by predators can address this structural issue with a mechanistic justification.

In both population-based and quantitative models, microbial predators increased equilibrium SOC stocks by reducing the abundance of decomposers. Models that lack explicit representation of top-down controls may incorporate their effects implicitly into other parameter values such as microbial biomass turnover rates or SOC pool decomposition rate constants. However, explicitly representing top-down control on microbial biomass facilitates examination of key parameter values across climates and ecosystems, allows for better mechanistic understanding of underlying processes, and draws a clearer link between model parameters and empirical estimates of biological processes. Our results further suggest that laboratory measurements of microbial biomass turnover rates in the absence of predators could underestimate microbial mortality relative to field conditions. Furthermore, the divergence of SOC temperature response (CE_a) from microbial temperature response as a function of predator traits in our results suggests that temperature response measurements of microbial physiology and enzymatic reaction rates may not be directly applicable to SOC decomposition rates.

Our results further suggest that not only the structure of the food web, but differences in the temperature dependence of species across trophic levels can determine the integrated response of the soil system to changes in temperature. As predators became more sensitive to temperature, SOC losses under warming weakened. Under some circumstances an increase in top-down control under warming could overwhelm increases in microbial substrate consumption rates and increase SOC stocks with warming. In a recent meta-analysis [6], 47% of soil warming manipulations observed increases in SOC rather than losses. Previous explanations for these unexpected results have included changes in soil moisture [59], increases in plant C inputs [60], and shifts in microbial physiology [8,61]. Our results suggest that increasing SOC under warming could also be explained by enhanced top-down control by microbial predators that increase their activity under warmer temperatures. Alternately, predators with low or negative thermal sensitivities could accelerate SOC losses under warming due to weakening of top-down control on microbial biomass. Our results also corroborate recent empirical studies indicating that temperature dependence of upper trophic levels could cascade down the soil food web, ultimately affecting soil respiration [39,42,62]. These results highlight the need to hone our understanding of how species respond to warming across soil trophic levels, instead of focusing only on the microbial decomposer component.

A significant challenge for this model structure is parameterization of processes related to trophic interactions [47]. Many important parameters in the models were poorly constrained in these simulations, including predator growth rates and CUE. Even parameters for which there is strong empirical evidence, such as thermal sensitivities, can vary substantially across organisms [63]. The high sensitivity of SOC temperature responses to the presence and traits of predators suggests that developing observational constraints for these parameters should be a priority in soil organic matter research. This said, note that

while our two modeling approaches share some core structural assumptions (two or three trophic levels, density-independent substrate inputs), they also incorporate substantially different assumptions (e.g., ratio-dependent predation vs ratio-independent predation, existence of multiple C types vs only one type of C) and have different parameterizations. Given these important differences, the level of congruence between the results of the two modeling approaches suggests that these qualitative results may apply broadly.

Global patterns of soil food web structure

Our results suggest that differential thermal sensitivities could drive differences in soil food web structure at different latitudes, depending on whether predator temperature traits are adapted to local climate. Top-down control on microbial populations was strongest in the tropics under globally-constant predator traits, while local temperature adaptation strengthened top-down control in colder regions. When predators were not adapted to local conditions, cold temperatures at high latitudes prevented predators from adopting a significant role. These results suggest that soil food web and decomposition responses to warming may be highly dependent on a combination of climate and local adaptation [64]. Because predator sensitivity to temperature mediates the response of the system to warming, food webs in different latitudes with different fauna or trophic structures are likely to have different warming responses.

Understanding differences in temperature sensitivity across trophic levels is thus crucial for projecting SOC responses to warming, given that temperature sensitivities are known to vary broadly across taxa, trophic levels, and habitats [63] and to differ among predators and their prey [63,65]. Temperature sensitivities are strongly correlated with body size [43], which could lead to different community responses depending on the size structure of trophic levels. For example, the predator trophic level in our model formulations could represent organisms like nematodes and amoebae, which, being larger than their bacterial and fungal prey, could suffer greater metabolic penalties from warming and thus realize lower biomass gains even with increasing consumption rates [43,66]. Alternately, top-down control could be exercised by viruses or phages, which are physically smaller and biochemically simpler than bacteria and fungi and, thus, might have very different thermal responses than larger organisms. A more sophisticated version of our modeling approach could include multiple organismal types at each trophic level, including decomposers with different traits (e.g., bacteria and fungi) and different types of predators with different traits and temperature sensitivities (e.g., phages, amoebae, nematodes, and microarthropods). Such a model might be more directly comparable with observations of soil biological communities but would introduce more difficult-to-constrain parameters.

Conclusions

Using two complementary modeling approaches, we show that the presence of a microbial predator decouples SOC temperature response from that of microbial decomposers by exerting top-down control on the latter. Our results suggest that SOC stocks are sensitive to food web structure, particularly the presence or absence of microbial predators, and that temperature sensitivity of decomposition is likely to be reduced by the presence of higher trophic levels. This effect ultimately depends on the relative temperature dependence of the microbial communities and their predators, which can lead to different responses across latitudes. This implies that measurements of temperature sensitivities should be understood in the context of broader trophic interactions before they can be directly applied to soil C decomposition and soil respiration parameters. Variations in temperature sensitivity across trophic levels

in soil food webs are therefore an important and underappreciated uncertainty in our predictive understanding of SOC dynamics and global change responses across climate zones and latitudes.

Acknowledgments

This material is based upon work supported by the U.S. Department of Energy, Office of Science, Office of Biological and Environmental Research as well as support from Duke University through startup funds. BNS thanks Asmeret Asefaw Berhe and the University of California, Merced for their support. We thank Aimée Classen and Debjani Sihi for helpful comments on the manuscript.

References

1. Jobbágy EG, Jackson RB. 2000 The vertical distribution of soil organic carbon and its relation to climate and vegetation. *Ecol. Appl.* **10**, 423–436. (doi:10.1890/1051-0761(2000)010[0423:TVDOSO]2.0.CO;2)
2. Crowther TW *et al.* 2016 Quantifying global soil carbon losses in response to warming. *Nature* **540**, 104–108. (doi:10.1038/nature20150)
3. Wieder WR, Hartman MD, Sulman BN, Wang Y-P, Koven CD, Bonan GB. 2018 Carbon cycle confidence and uncertainty: Exploring variation among soil biogeochemical models. *Glob. Chang. Biol.* **24**, 1563–1579. (doi:10.1111/gcb.13979)
4. Todd-Brown KEO *et al.* 2014 Changes in soil organic carbon storage predicted by Earth system models during the 21st century. *Biogeosciences* **11**, 2341–2356. (doi:10.5194/bg-11-2341-2014)
5. van Gestel N *et al.* 2018 Predicting soil carbon loss with warming. *Nature* **554**, E4–E5. (doi:10.1038/nature25745)
6. Sulman BN *et al.* 2018 Multiple models and experiments underscore large uncertainty in soil carbon dynamics. *Biogeochemistry* **141**, 109–123. (doi:10.1007/s10533-018-0509-z)
7. Wieder WR *et al.* 2015 Explicitly representing soil microbial processes in Earth system models. *Global Biogeochem. Cycles* **29**. (doi:10.1002/2015GB005188)
8. Allison SD, Wallenstein MD, Bradford MA. 2010 Soil-carbon response to warming dependent on microbial physiology. *Nat. Geosci.* **3**, 336–340.
9. Wieder WR, Bonan GB, Allison SD. 2013 Global soil carbon projections are improved by modelling microbial processes. *Nat. Clim. Chang.* **3**, 909–912. (doi:10.1038/nclimate1951)
10. Sulman BN, Phillips RP, Oishi AC, Shevliakova E, Pacala SW. 2014 Microbe-driven turnover offsets mineral-mediated storage of soil carbon under elevated CO2. *Nat. Clim. Chang.* **4**, 1099–1102. (doi:10.1038/nclimate2436)
11. Wang G, Mayes MA, Gu L, Schadt CW. 2014 Representation of Dormant and Active Microbial Dynamics for Ecosystem Modeling. *PLoS One* **9**, e89252. (doi:10.1371/journal.pone.0089252)
12. Salazar A, Sulman BN, Dukes JS. 2018 Microbial dormancy promotes microbial biomass and respiration across pulses of drying-wetting stress. *Soil Biol. Biochem.* **116**, 237–244. (doi:10.1016/j.soilbio.2017.10.017)
13. Georgiou K, Abramoff RZ, Harte J, Riley WJ, Torn MS. 2017 Microbial community-level regulation explains soil carbon responses to long-term litter manipulations. *Nat. Commun.* **8**, 1–10. (doi:10.1038/s41467-017-01116-z)
14. Wieder WR, Grandy AS, Kallenbach CM, Taylor PG, Bonan GB. 2015 Representing life in the Earth system with soil microbial functional traits in the MIMICS model. *Geosci. Model Dev.* **8**, 1789–1808. (doi:10.5194/gmd-8-1789-2015)

15. Huang Y, Guenet B, Ciais P, Janssens IA, Soong JL, Wang Y, Goll D, Blagodatskaya E, Huang Y. 2018 ORCHIMIC (v1.0), a microbe-mediated model for soil organic matter decomposition. *Geosci. Model Dev.* **11**, 2111–2138. (doi:10.5194/gmd-11-2111-2018)
16. Wang Y-PP *et al.* 2014 Oscillatory behavior of two nonlinear microbial models of soil carbon decomposition. *Biogeosciences* **11**, 1817–1831. (doi:10.5194/bg-11-1817-2014)
17. Sihi D, Gerber S, Inglett PW, Inglett KS. 2016 Comparing models of microbial–substrate interactions and their response to warming. *Biogeosciences* **13**, 1733–1752. (doi:10.5194/bg-13-1733-2016)
18. Manzoni S, Taylor P, Richter A, Porporato A, Ågren GI. 2012 Environmental and stoichiometric controls on microbial carbon-use efficiency in soils. *New Phytol.* **196**, 79–91. (doi:10.1111/j.1469-8137.2012.04225.x)
19. Wallenstein MD, Weintraub MN. 2008 Emerging tools for measuring and modeling the in situ activity of soil extracellular enzymes. *Soil Biol. Biochem.* **40**, 2098–2106. (doi:10.1016/J.SOILBIO.2008.01.024)
20. Allison SD, Martiny JBH. 2008 Resistance, resilience, and redundancy in microbial communities. *Proc. Natl. Acad. Sci.* **105**, 11512–11519. (doi:10.1073/pnas.0801925105)
21. Trivedi P, Anderson IC, Singh BK. 2013 Microbial modulators of soil carbon storage: integrating genomic and metabolic knowledge for global prediction. *Trends Microbiol.* **21**, 641–651. (doi:10.1016/J.TIM.2013.09.005)
22. Bailey VL *et al.* 2018 Soil carbon cycling proxies: Understanding their critical role in predicting climate change feedbacks. *Glob. Chang. Biol.* **24**, 895–905. (doi:10.1111/gcb.13926)
23. Buchkowski RW, Bradford MA, Grandy AS, Schmitz OJ, Wieder WR. 2017 Applying population and community ecology theory to advance understanding of belowground biogeochemistry. *Ecol. Lett.* **20**, 231–245. (doi:10.1111/ele.12712)
24. Grandy AS, Wieder WR, Wickings K, Kyker-Snowman E. 2016 Beyond microbes: Are fauna the next frontier in soil biogeochemical models? *Soil Biol. Biochem.* **102**, 40–44. (doi:10.1016/J.SOILBIO.2016.08.008)
25. Soong JL, Nielsen UN. 2016 The role of microarthropods in emerging models of soil organic matter. *Soil Biol. Biochem.* **102**, 37–39. (doi:10.1016/j.soilbio.2016.06.020)
26. Bonkowski M. 2004 Protozoa and plant growth: the microbial loop in soil revisited. *New Phytol.* **162**, 617–631. (doi:10.1111/j.1469-8137.2004.01066.x)
27. Brussaard L. 1998 Soil fauna, guilds, functional groups and ecosystem processes. *Appl. Soil Ecol.* **9**, 123–135. (doi:10.1016/S0929-1393(98)00066-3)
28. Carpenter SR, Kitchell JF, Hodgson JR. 1985 Cascading Trophic Interactions and Lake Productivity. *Bioscience* **35**, 634–639. (doi:10.2307/1309989)
29. Dell AI, Pawar S, Savage VM. 2014 Temperature dependence of trophic interactions are driven by asymmetry of species responses and foraging strategy. *J. Anim. Ecol.* (doi:10.1111/1365-2656.12081)
30. Gilbert B *et al.* 2014 A bioenergetic framework for the temperature dependence of trophic interactions. *Ecol. Lett.* (doi:10.1111/ele.12307)
31. Pawar S, Dell AI, Savage VM, Knies JL. 2016 Real versus Artificial Variation in the Thermal Sensitivity of Biological Traits. *Am. Nat.* (doi:10.1086/684590)
32. Gibert JP, Chelini MC, Rosenthal MF, Delong JP. 2016 Crossing regimes of temperature dependence in animal movement. *Glob. Chang. Biol.* (doi:10.1111/gcb.13245)
33. Gibert JP, DeLong JP. 2017 Phenotypic variation explains food web structural patterns. *Proc. Natl. Acad. Sci.* **114**, 201703864. (doi:10.1073/pnas.1703864114)
34. Ozgul A, Tuljapurkar S, Benton TG, Pemberton JM, Clutton-Brock TH, Coulson T. 2009 The Dynamics of Phenotypic Change and the Shrinking Sheep of St. Kilda. *Science (80-.).* **325**, 464–467. (doi:10.1126/science.1173668)
35. Ozgul A, Childs DZ, Oli MK, Armitage KB, Blumstein DT, Olson LE, Tuljapurkar S, Coulson T. 2010 Coupled dynamics of body mass and population growth in response to environmental

change. *Nature* (doi:10.1038/nature09210)
36. Reynolds PL *et al.* 2018 Latitude, temperature, and habitat complexity predict predation pressure in eelgrass beds across the Northern Hemisphere. *Ecology* **99**, 29–35. (doi:10.1002/ecy.2064)
37. Romero GQ, Piccoli GCO, de Omena PM, Gonçalves-Souza T. 2016 Food web structure shaped by habitat size and climate across a latitudinal gradient. *Ecology* **97**, 2705–2715. (doi:10.1002/ecy.1496)
38. O'Connor MI. 2009 Warming strengthens an herbivore–plant interaction. *Ecology* **90**, 388–398. (doi:10.1890/08-0034.1)
39. Crowther TW, Thomas SM, Maynard DS, Baldrian P, Covey K, Frey SD, van Diepen LTA, Bradford MA. 2015 Biotic interactions mediate soil microbial feedbacks to climate change. *Proc. Natl. Acad. Sci.* **112**, 7033–7038. (doi:10.1073/pnas.1502956112)
40. Frey SD, Gupta V, Elliott ET, Paustian K. 2001 Protozoan grazing affects estimates of carbon utilization efficiency of the soil microbial community. *Soil Biol. Biochem.* **33**, 1759–1768.
41. Bradford MA *et al.* 2007 Carbon dynamics in a model grassland with functionally different soil communities. *Funct. Ecol.* **21**, 690–697. (doi:10.1111/j.1365-2435.2007.01268.x)
42. Koltz AM, Classen AT, Wright JP. 2018 Warming reverses top-down effects of predators on belowground ecosystem function in Arctic tundra. *Proc. Natl. Acad. Sci.* , 201808754. (doi:10.1073/pnas.1808754115)
43. Brose U, Dunne JA, Montoya JM, Petchey OL, Schneider FD, Jacob U. 2012 Climate change in size-structured ecosystems. *Philos. Trans. R. Soc. B Biol. Sci.* **367**, 2903–2912. (doi:10.1098/rstb.2012.0232)
44. Petchey OL, McPhearson PT, Casey TM, Morin PJ. 1999 Environmental warming alters food-web structure and ecosystem function. *Nature* **402**, 69–72. (doi:10.1038/47023)
45. Gibert JP. 2019 Temperature directly and indirectly influences food web structure. *Sci. Rep.* **9**, 5312. (doi:10.1038/s41598-019-41783-0)
46. Osler GHR, Sommerkorn M. 2007 Toward a complete soil C and N cycle: Incorporating the soil fauna. *Ecology* **88**, 1611–1621. (doi:10.1890/06-1357.1)
47. Smith P, Andrén O, Brussaard L, Dangerfield M, Ekschmitt K, Lavelle P, Tate K. 1998 Soil biota and global change at the ecosystem level: describing soil biota in mathematical models. *Glob. Chang. Biol.* **4**, 773–784. (doi:10.1046/j.1365-2486.1998.00193.x)
48. Todd-Brown KEO, Randerson JT, Post WM, Hoffman FM, Tarnocai C, Schuur EAG, Allison SD. 2013 Causes of variation in soil carbon simulations from CMIP5 Earth system models and comparison with observations. *Biogeosciences* **10**, 1717–1736.
49. Rosenzweig ML, MacArthur RH. 1963 Graphical Representation and Stability Conditions of Predator-Prey Interactions. *Am. Nat.* (doi:10.1086/282272)
50. Binzer A, Guill C, Brose U, Rall BC. 2012 The dynamics of food chains under climate change and nutrient enrichment. *Philos. Trans. R. Soc. B Biol. Sci.* **367**, 2935–2944. (doi:10.1098/rstb.2012.0230)
51. Osmond MM, Barbour MA, Bernhardt JR, Pennell MW, Sunday JM, O'Connor MI. 2017 Warming-Induced Changes to Body Size Stabilize Consumer-Resource Dynamics. *Am. Nat.* **189**, 718–725. (doi:10.1086/691387)
52. Sollins P, Homann P, Caldwell BA. 1996 Stabilization and destabilization of soil organic matter: Mechanisms and controls. *Geoderma* **74**, 65–105.
53. Hicks Pries CE *et al.* 2018 Root litter decomposition slows with soil depth. *Soil Biol. Biochem.* **125**, 103–114. (doi:10.1016/j.soilbio.2018.07.002)
54. Shevliakova E *et al.* 2009 Carbon cycling under 300 years of land use change: Importance of the secondary vegetation sink. *Global Biogeochem. Cycles* **23**, n/a-n/a. (doi:10.1029/2007GB003176)
55. Milly PCD *et al.* 2014 An enhanced model of land water and energy for global hydrologic and earth-system studies. *J. Hydrometeorol.* **15**, 1739–1761.
56. Sheffield J, Goteti G, Wood EF. 2006 Development of a 50-Year High-Resolution Global Dataset of Meteorological Forcings for Land Surface Modeling. *J. Clim.* **19**, 3088–3111.

(doi:10.1175/JCLI3790.1)
57. Sulman BN, Brzostek ER, Medici C, Shevliakova E, Menge DNL, Phillips RP. 2017 Feedbacks between plant N demand and rhizosphere priming depend on type of mycorrhizal association. *Ecol. Lett.* **20**, 1043–1053. (doi:10.1111/ele.12802)
58. Todd-Brown K, Zheng B, Crowther TW. 2018 Field-warmed soil carbon changes imply high 21st-century modeling uncertainty. *Biogeosciences* **15**, 3659–3671. (doi:10.5194/bg-15-3659-2018)
59. Saleska SR, Harte J, Torn MS. 1999 The effect of experimental ecosystem warming on CO2 fluxes in a montane meadow. *Glob. Chang. Biol.* **5**, 125–141. (doi:10.1046/j.1365-2486.1999.00216.x)
60. Lu M, Zhou X, Yang Q, Li H, Luo Y, Fang C, Chen J, Yang X, Li B. 2013 Responses of ecosystem carbon cycle to experimental warming: A meta-analysis. *Ecology* **94**, 726–738. (doi:10.1890/12-0279.1)
61. Bradford MA, Davies CA, Frey SD, Maddox TR, Melillo JM, Mohan JE, Reynolds JF, Treseder KK, Wallenstein MD. 2008 Thermal adaptation of soil microbial respiration to elevated temperature. *Ecol. Lett.* **11**, 1316–1327. (doi:10.1111/j.1461-0248.2008.01251.x)
62. Ruess L, Michelsen A, Schmidt IK, Jonasson S. 2017 Simulated climate change affecting microorganisms, nematode density and biodiversity in subarctic soils. **212**, 63–73. (doi:10.1023/A:1004567816355)
63. Dell AI, Pawar S, Savage VM. 2011 Systematic variation in the temperature dependence of physiological and ecological traits. *Proc. Natl. Acad. Sci.* **108**, 10591–10596. (doi:10.1073/pnas.1015178108)
64. Tylianakis JM, Didham RK, Bascompte J, Wardle DA. 2008 Global change and species interactions in terrestrial ecosystems. *Ecol. Lett.* **11**, 1351–1363. (doi:10.1111/j.1461-0248.2008.01250.x)
65. Voigt W *et al.* 2003 Trophic levels are differentially sensitive to climate. *Ecology* **84**, 2444–2453. (doi:10.1890/02-0266)
66. Lang B, Ehnes RB, Brose U, Rall BC. 2017 Temperature and consumer type dependencies of energy flows in natural communities. *Oikos* **126**, 1717–1725. (doi:10.1111/oik.04419)

Figures

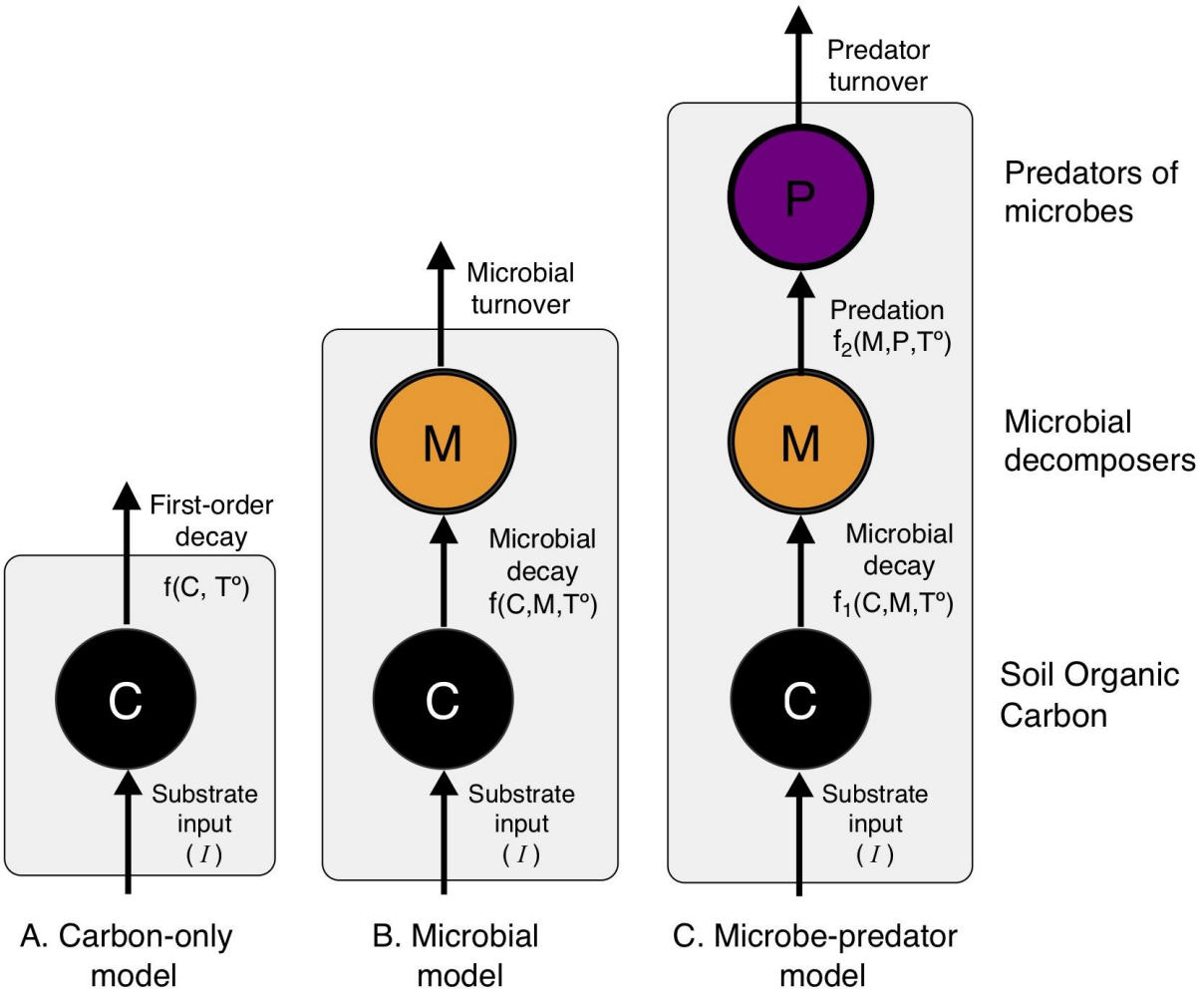

Figure 1: Diagram of three approaches to SOC modeling. A first-order model has only one trophic level (SOC). A microbial model adds a second trophic level, and a microbe-predator model includes a third trophic level. Transfers from one level to the next are mediated by temperature and population of adjacent trophic levels.

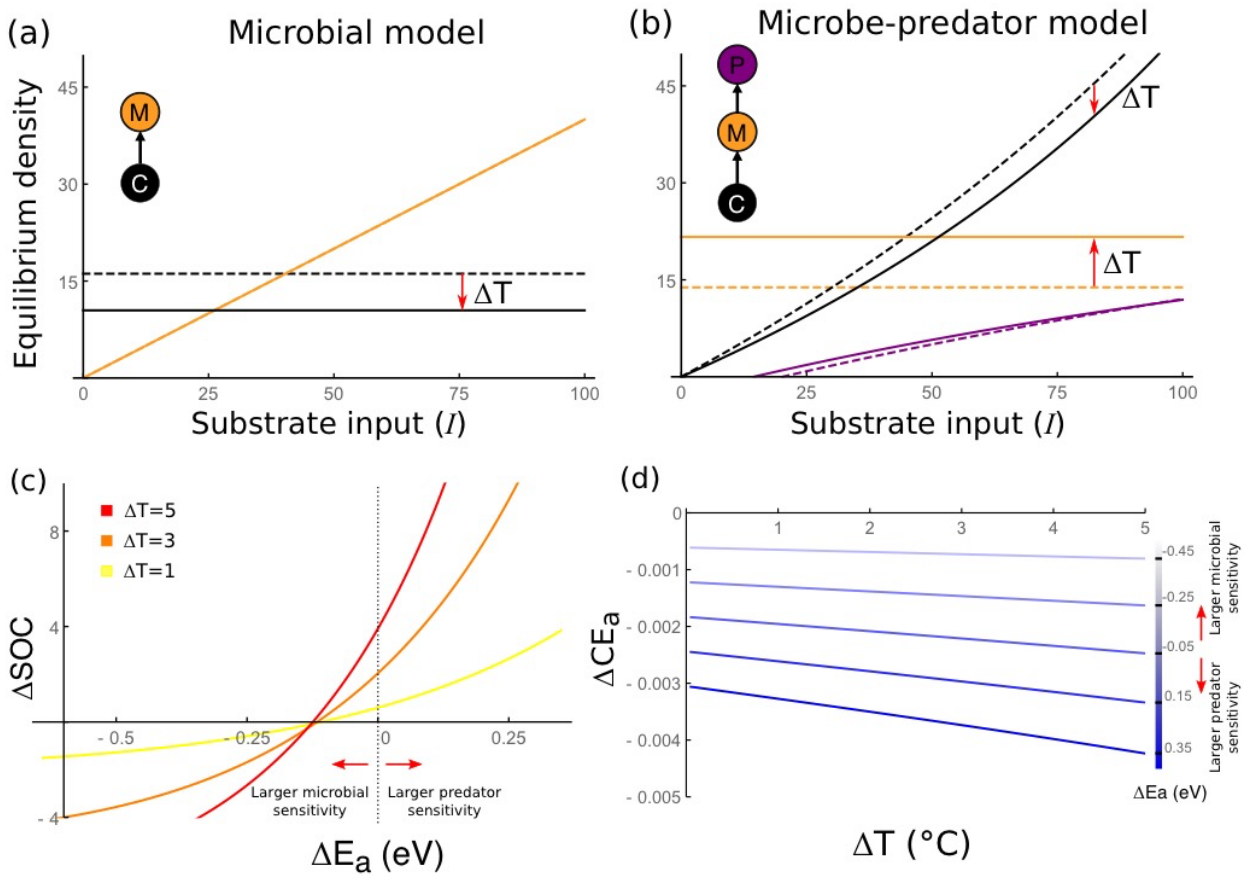

Figure 2: Equilibrium densities of substrate (C), microbes (M), and predators (P) of population-based microbial (a) and microbe-predator (b) models over a range of substrate input rates and two temperatures. Dashed lines show simulations at 20 ºC and solid lines show simulations at 25 ºC. (c) Effect of relative microbial and predator temperature sensitivities on equilibrium SOC response to warming (relative to 20 ºC). ΔEa is the difference between microbial and predator Ea parameters in electron-volts. (d) Difference in the temperature sensitivity of SOC between a three-level model (with predators) and a two-level model (without predators) at different levels of warming (as ΔT over ambient), for differences in temperature sensitivities between predators and microbes (blue-color coded).

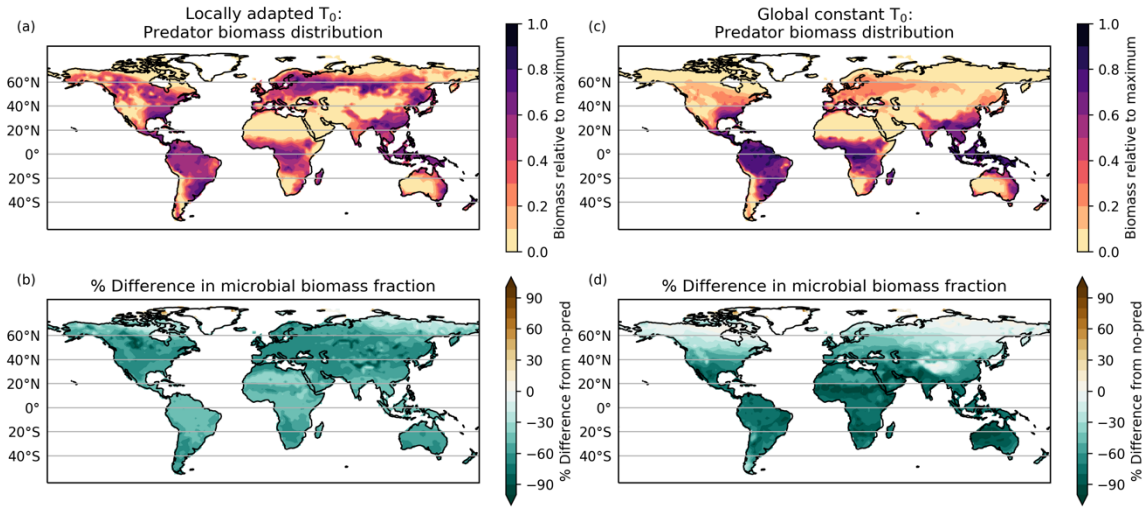

Figure 3: Predator biomass distribution and impacts on microbial biomass at steady state. Panels a and b show simulations with locally-adapted predator T_0, and panels c and d show simulations with constant global T_0. Panels a and c show total simulated predator biomass carbon, and panels b and d show the percent difference in microbial biomass expressed as a fraction of total SOC compared to control simulations.

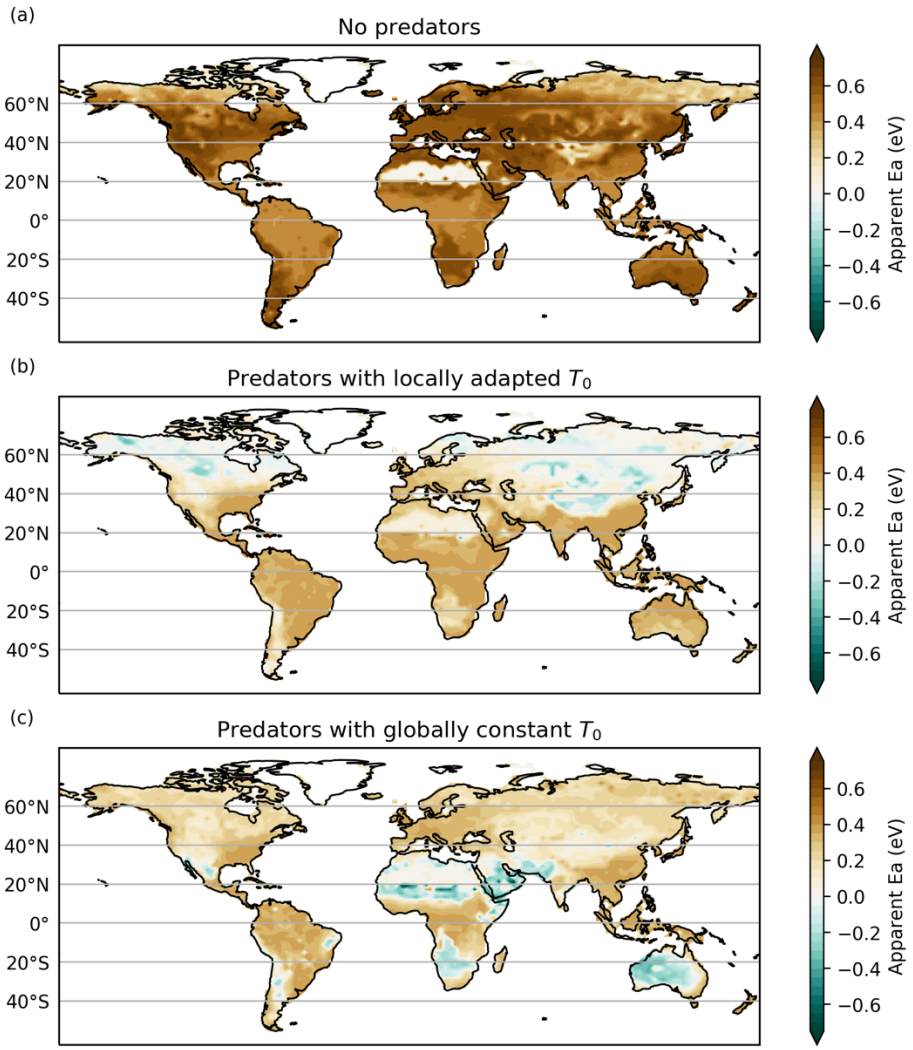

Figure 4: CE_a of unprotected SOC stocks under alternative assumptions of predator traits. (a): CORPSE model without predators. (b): Predators with T_0 equal to mean annual temperature in each grid cell, representing local adaptation. (c): Predators with a single global T_0 equal to global mean temperature.

Supplemental Material

First order and Microbial models

The simplest approach to modeling SOC decomposition only considers carbon stock (C) naturally decaying over time at a temperature-dependent first-order rate k (Fig 1A) while being replenished at a constant rate I:

$$\frac{dC}{dt} = I - k(T)C \quad \text{(S1)}$$

Here, we model the microbial effect on carbon as a classic type-II predator functional response, where the SOC decomposition rate depends on microbial biomass and carbon stocks (M and C, respectively), as well as on two parameters controlling the feeding process, the microbial attack rate (α) and handling time η [1,2]. We further assume that the conversion of carbon into microbial biomass is determined by a conversion efficiency parameter (ε), that carbon stocks are replenished at a constant rate I, determined by substrate input levels, and that microbes die naturally at a per-capita rate d_M. For simplicity, we assume that microbial deaths do not feed back into the SOC pool, but such a scenario can be taken into account by slightly altering substrate input levels. Together, the model calculates the rates of change of C stocks and M biomass over time through the following system of differential equations:

$$\frac{dC}{dt} = I - \frac{\alpha(T)CM}{1+\alpha(T)\eta C} \quad \text{(S2)}$$

$$\frac{dM}{dt} = \varepsilon\frac{\alpha(T)CM}{1+\alpha(T)\eta C} - d_M M \quad \text{(S3)}$$

We further modified this model by assuming, for simplicity, that microbial attack rates, but no other model parameters, are temperature-dependent, following an Arrhenius function of the form:

$$\alpha(T) = Ve^{-\frac{E_a}{k_b}\left(\frac{1}{T}-\frac{1}{T_0}\right)}, \quad \text{(S4)}$$

where V is a pre-exponential rate constant (units of inverse time), k_b is the Boltzmann constant ($8.62\text{x}10^{-5}$ electron-volts per degree Kelvin, eV K^{-1}), T is the temperature at which the process occurs (in K), T_0 is a reference temperature (K), and E_a is the activation energy of the process (in eV), which is a measure of its temperature dependence [3–5].

CORPSE-Pred Model Equations

The soil carbon model is an adaptation of the Carbon Organisms Rhizosphere and Protection in the Soil Environment (CORPSE) model (Sulman et al, 2014), modified to allow tracking of carbon isotopes. Organic matter is divided into three chemically-defined forms, which can be either protected or unprotected. Protected organic matter is inaccessible to microbial decomposition through chemical sorption to mineral surfaces or occlusion within micro-aggregates. Unprotected organic matter can be added as litter or root exudate inputs, decomposed by microbial action, or protected:

$$\frac{dC_{U,i}}{dt} = I_{C,i} - D_i + T_M + T_P - \frac{dC_{P,i}}{dt} \quad (1)$$

where $C_{U,i}$ is unprotected C; $I_{C,i}$ is external inputs of C (including litter deposition and root exudation); $D_{i,j}$ is decomposition rate; T_M is microbial necromass production; T_P is predator necromass production; and $\frac{dC_{P,i}}{dt}$ is net transfer of C to or from the protected state. *i* refers to chemically-defined types, which can be chemically simple plant-derived material (representing compounds like glucose or amino acids that are readily decomposed), chemically resistant (representing compounds like lignin or complex microbially-produced chemicals), or readily decomposable microbial and predator necromass.

Protected C is formed from unprotected organic matter and converted back to unprotected form at first-order rates:

$$\frac{dC_{P,i}}{dt} = C_{U,i} \cdot \gamma_i - \frac{C_{P,i}}{\tau_{C_P}} \quad (2)$$

The decomposition flux is controlled by microbial biomass (B_M), temperature (T), and volumetric soil water content (θ):

$$D_i = V_{max,i}(T) \cdot \left(\frac{\theta}{\theta_{sat}}\right)^a \left(1 - \frac{\theta}{\theta_{sat}}\right)^b \cdot C_i \frac{M/C_i}{M/C_i + k_M} \quad (3)$$

where $\theta_{sat}$is the saturation level of θ. Note that decomposition rate is controlled by the ratio of total microbial biomass carbon (summed over isotope fractions) to substrate carbon (also summed over isotope fractions) on a substrate-specific basis. The maximum decomposition rate is controlled by the Arrhenius relationship, which describes the temperature dependence of enzymatic reactions:

$$V_{max,i}(T) = V_{max,ref,i} \times \exp\left(-\frac{E_{a,i}}{RT}\right) \quad (4)$$

where $V_{max,ref,i}$ is a maximum decomposition rate specific to each chemically-defined organic matter type, $E_{a,i}$ is activation energy for each organic matter type, and R is the ideal gas constant (8.31 J K^{-1} mol^{-1}).

Microbial growth is supported by uptake of decomposed organic matter, and biomass is lost through turnover at a fixed rate:

$$\frac{dB_M}{dt} = \sum_i (D_i CUE_i) - \max\left(M - M_{min} \cdot \sum_i C_{U,i}, 0\right) d_M - p \quad (5)$$

Where M_{min} is minimum microbial biomass expressed as a fraction of total unprotected C and p is predation rate. Turnover is divided into maintenance respiration, which is converted directly to CO_2, and necromass production. The division between maintenance and respiration and necromass production is controlled by a parameter ϵ_t:

$$R_{maint} = \max\left(M - M_{min} \cdot \sum_i C_{U,i}, 0\right) d_M (1 - \epsilon_t) \quad (6)$$

$$T_{M,j} = \max\left(M - M_{min} \cdot \sum_i C_{U,i}, 0\right) d_M \, (\epsilon_t) \quad (7)$$

Predation rate is similar to decomposition rate, but controlled by predator biomass and, for simplicity, assumed to be independent of soil moisture:

$$p = V_{max,P}(T) M \frac{P/M}{P/M + k_P} \quad (8)$$

$$V_{max,P}(T) = V_{max,ref,P} \times \exp\left(-\frac{E_{a,P}}{RT}\right) \quad (9)$$

And predator growth and turnover are similar to their microbial counterparts, but depending on microbial biomass rather than substrate C:

$$\frac{dP}{dt} = p \cdot CUE_P - \max\left(P - P_{min} \cdot M, 0\right) d_P \quad (10)$$

Where CUE_P is predator carbon use efficiency, P_{min} is minimum predator biomass as a fraction of microbial biomass, and τ_P is turnover time of predator biomass. As with microbes, predator biomass turnover is divided into necromass production and maintenance respiration:

$$R_{maint,P} = \max\left(P - P_{min} \cdot M, 0\right) d_P \left(1 - \epsilon_{t,P}\right) \quad (11)$$

$$T_P = \max\left(P - P_{min} \cdot M, 0\right) d_P \left(\epsilon_{t,P}\right) \quad (12)$$

Total CO_2 production rate is the sum of maintenance respiration and respiration derived from decomposition processes:

$$\frac{dCO_2}{dt} = R_{maint} + R_{maint,P} + \sum_i ((1 - CUE_i) D_i) + (1 - CUE_P \cdot p) \quad (13)$$

References

1. Rosenzweig ML, MacArthur RH. 1963 Graphical Representation and Stability Conditions of Predator-Prey Interactions. *Am. Nat.* (doi:10.1086/282272)
2. Binzer A, Guill C, Brose U, Rall BC. 2012 The dynamics of food chains under climate change and nutrient enrichment. *Philos. Trans. R. Soc. B Biol. Sci.* **367**, 2935–2944. (doi:10.1098/rstb.2012.0230)
3. Gilbert B *et al.* 2014 A bioenergetic framework for the temperature dependence of trophic interactions. *Ecol. Lett.* (doi:10.1111/ele.12307)
4. Osmond MM, Barbour MA, Bernhardt JR, Pennell MW, Sunday JM, O'Connor MI. 2017 Warming-Induced Changes to Body Size Stabilize Consumer-Resource Dynamics. *Am. Nat.* **189**, 718–725. (doi:10.1086/691387)
5. Gibert JP, Chelini MC, Rosenthal MF, Delong JP. 2016 Crossing regimes of temperature dependence in animal movement. *Glob. Chang. Biol.* (doi:10.1111/gcb.13245)

713 Model parameters

714 Table S1: Parameter values for the population-based models used in Figure 2.

Parameter	Description	Value	Units
η_1	Microbial handling time	0.04	Time
η_2	Predator handling time	0.04	Time
ε_1	Microbial conversion efficiency	0.4	Unitless
ε_2	Predator conversion efficiency	0.2	Unitless
d_M	Microbial death rate	1.0	$Time^{-1}$
d_P	Predator death rate	0.8	$Time^{-1}$
V_1	Microbial attack rate	0.22	$Time^{-1}$
V_2	Predator attack rate	0.22	$Time^{-1}$
Ea_1	Microbial activation energy	0.65	eV
Ea_2	Predator activation energy	0.65	eV
T_0	Reference temperature	15	ºC

715

716 Table S2: CORPSE-Pred parameters

Parameter	Description	Value	Units
V_1	Max decomposition rate for simple C	9.0	$year^{-1}$
V_2	Max decomposition rate for complex C	0.25	$year^{-1}$
V_3	Max decomposition rate for necromass C	4.5	$year^{-1}$
Ea_1	Activation energy for simple C	0.052	eV
Ea_2	Activation energy for complex C	0.31	eV
Ea_3	Activation energy for necromass C	0.052	eV
k_M	Microbial decomposition saturation parameter	0.1	g microbial C g substrate C^{-1}

a	Moisture sensitivity parameter	1.5	Unitless
b	Moisture sensitivity parameter	0.6	Unitless
M_{min}	Minimum microbial biomass	0.001	g microbial C g substrate C^{-1}
d_M	Microbial death rate	4.0	$year^{-1}$
ε_1	Microbial conversion efficiency for simple C	0.6	Unitless
ε_2	Microbial conversion efficiency for complex C	0.05	Unitless
ε_3	Microbial conversion efficiency for necromass C	0.6	Unitless
γ_1	Protection rate of simple C	0.3	$year^{-1}$
γ_2	Protection rate of complex C	0.001	$year^{-1}$
γ_3	Protection rate of necromass C	1.5	$year^{-1}$
τ_{C_P}	Turnover time of protected C	75	years
V_P	Max predation rate	4.0	$year^{-1}$
Ea_P	Predator activation energy	0.31	eV
P_{min}	Minimum predator C	0.001	g predator C g microbial C^{-1}
d_P	Predator death rate	2.0	$year^{-1}$
ε_P	Predator conversion efficiency	0.5	Unitless
k_P	Predation saturation parameter	0.5	g predator C g microbial C^{-1}

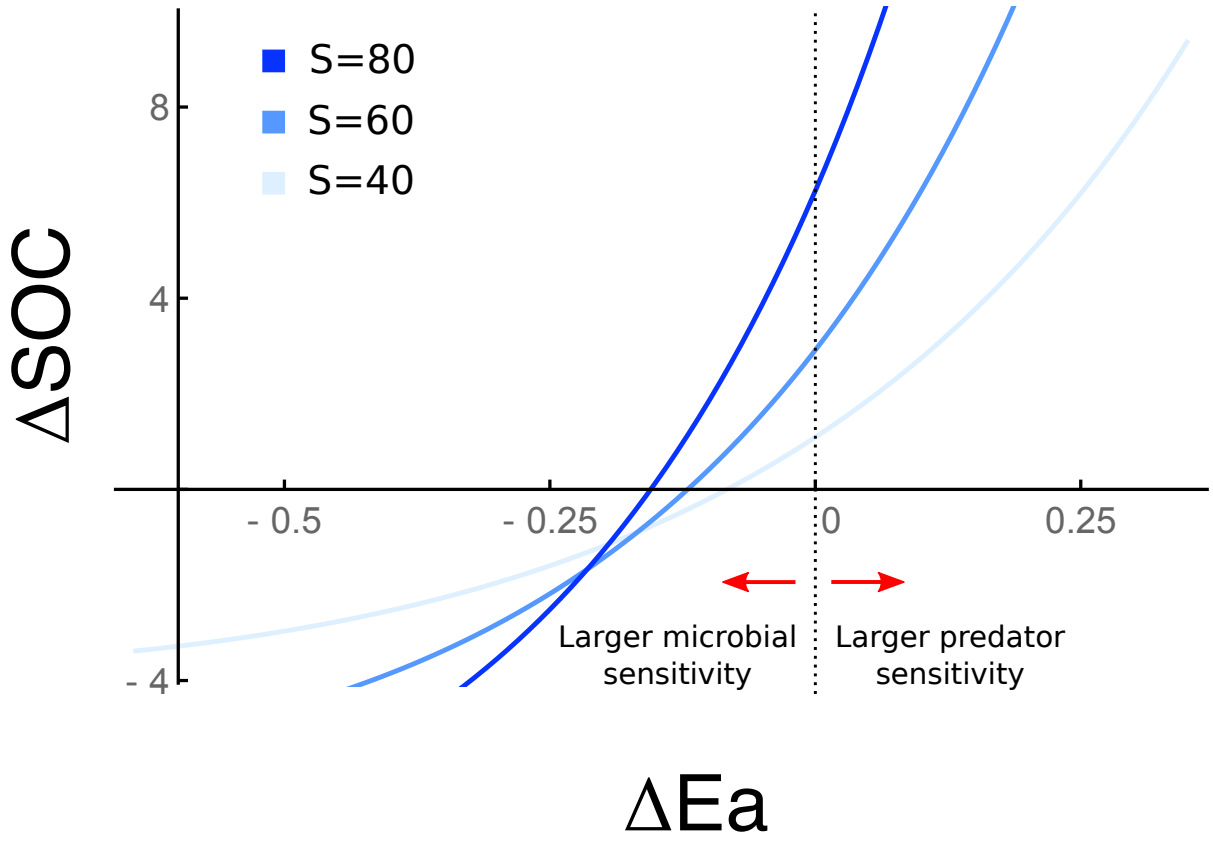

Figure S1: Change in steady-state SOC stock under 4ºC warming as a function of predator Ea, for three different substrate input rates using the population-based model.

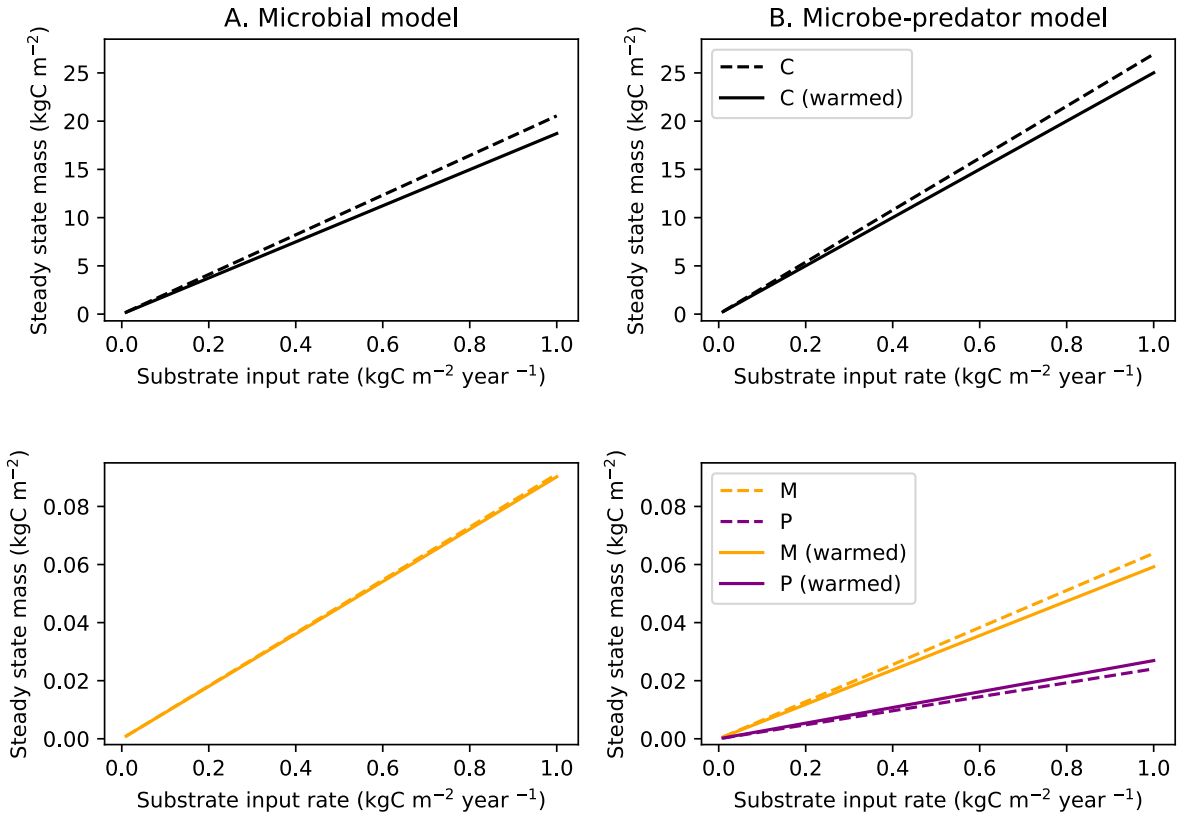

Figure S2: Model pools as a function of substrate input using CORPSE-Pred. These plots are comparable to Fig. 2 in the main text. Microbial and predator pools are shown separately from SOC for better visibility due to the large differences in stock magnitudes.

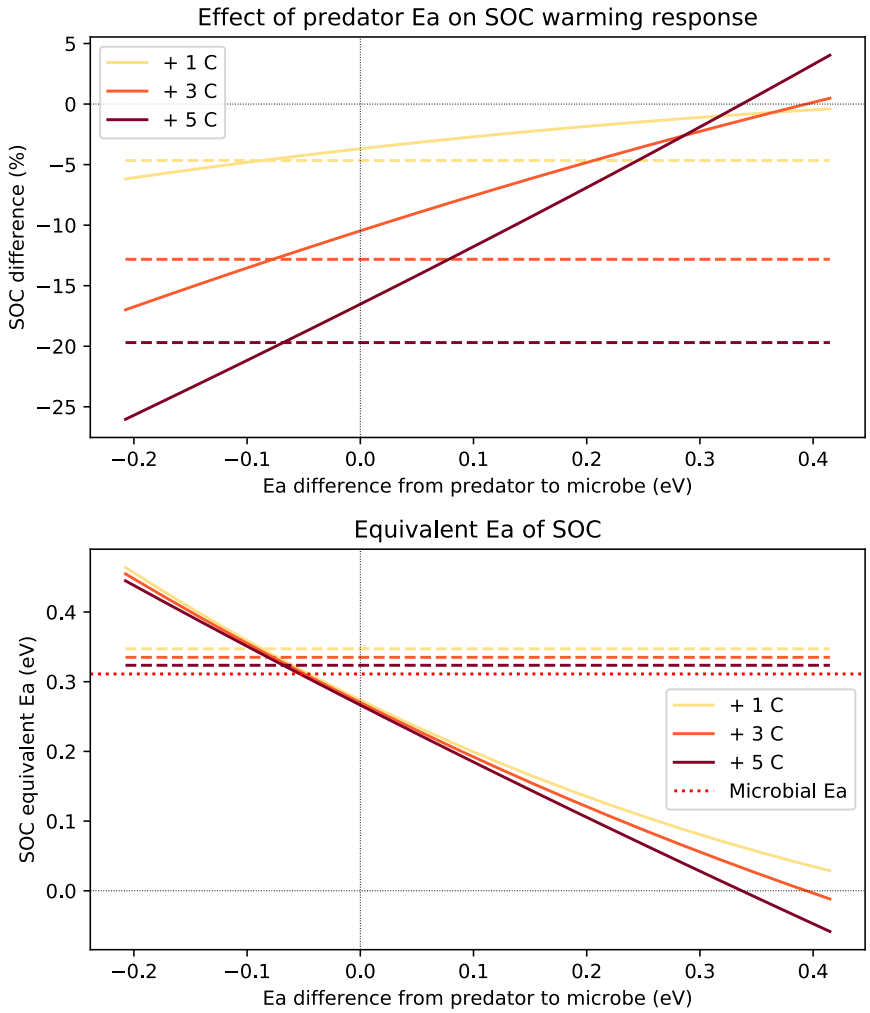

735

736 Figure S3: (a) Effect of relative microbial and predator temperature sensitivities on equilibrium SOC
737 response to warming, using CORPSE-Pred model. Dashed lines show simulations without predators. This
738 figure is comparable to Fig. 2c in the main text. (b) Data from the top panel expressed as *CEa*. Dashed
739 lines show simulations without predators, and dotted red line shows the actual *Ea* parameter value of the
740 slow-cycling component of unprotected SOC.

741